RSC Advances

PAPER

View Article Online
View Journal | View Issue

Cite this: *RSC Adv.*, 2017, **7**, 18500

Development of a compact MnO_2 filter for removal of SO_2 from diesel vehicle emissions

Xuecheng Liu,[ab] Yugo Osaka,[c] Hongyu Huang,[*a] Jun Li,[*d] Zhaohong He,[a] Xixian Yang,[a] Huhetaoli,[a] Shijie Li[a] and Noriyuki Kobayashi[d]

Received 4th January 2017
Accepted 22nd March 2017

DOI: 10.1039/c7ra00096k

rsc.li/rsc-advances

Increasing concern about sulfur dioxide (SO_2) from diesel vehicle exhausts causing detrimental effects on NO_x removal catalysts has resulted in the development of dry desulfurization filters for complete removal of SO_2. In this study, a compact MnO_2 filter was developed for diesel emission control. The SO_2-capture behavior of the compact MnO_2 filter was investigated by using a volumetric device in a low temperature range (200–400 °C) and low SO_2 pressure conditions. The maximal capacity of the MnO_2 filter was 304.1 mg_{SO_2} per g_{MnO_2} at 400 °C. Based on the experimental results, the required volume of the MnO_2 filter was estimated as only 0.6 L for a diesel car with 30 000 km distance traveled per year. The thickness of the MnO_2 filter had significant influence on its SO_2-capture performance. The sulfate reaction mechanism was also discussed by using a grain model under four reaction temperature conditions for improving the efficiency of the design of the desulfurization filter. The sulfate process can be divided into two control stages (the chemical reaction control stage and the solid diffusion control stage) and the prediction models fit the experimental data well for both control stages, indicating that the two-stage grain model is suitable for the sulfate reaction between the MnO_2 filter and SO_2. The calculated apparent activation energy of 18.8 kJ mol^{-1} indicates that the MnO_2 filter exhibits high activity for SO_2 adsorption in a pure SO_2 atmosphere.

Introduction

The removal of sulfur dioxide (SO_2) from vehicle exhausts is of great interest for the reason that SO_2 has detrimental effects on human health and the environment.[1,2] Besides, SO_2 from diesel vehicle exhaust gas greatly deactivates the NO_x removal catalysts because sulfates are more stable than nitrates.[3] Compared with the flue gas from large power plants, diesel exhaust gas is quite different because of the low emission amounts, wide temperature range, high space velocity and low sulfur concentration (the sulfur content of diesel varying from tens of ppm to hundreds of ppm). Therefore the traditional wet flue gas desulfurization technologies for large power plants are not suitable for diesel exhaust systems. To solve the issues caused by SO_2 emissions from diesel exhausts, compact SO_2 traps of dry desulfurization technologies have been proposed for complete capture of SO_2 from diesel vehicle exhausts.[4–7]

The traditional dry desulfurization materials, such as calcined limestone[8] and $CaCO_3$ materials,[9] have good sulfate reactivity over 650 °C with high SO_2 concentration over 1000 ppm. However, SO_2 capture capacity of these materials declines sharply below 400 °C because the sulfate reaction activity is limited by the decarbonation.[9] With continuous development of the diesel engine technology, the maximum temperature of diesel exhaust will be decreased to 400 °C. Therefore the development of low-temperature activation and downsizing of the compact SO_2 trap is needed for mounting on mobile diesel vehicle.

To enhance the low-temperature SO_2-capture performance of desulfurization materials, Rubio and Izquierdo[10] studied the SO_2 removal performance of coal fly ash based carbons at flue gas conditions and the amount of SO_2 removed is 13 mg g^{-1} by the Lada activated sample at 100 °C and 1000 ppmv SO_2 gas conditions. The SO_2 oxidation activity of copper oxide supported on the activated carbon could be improved at low temperature at 250 °C.[11,12] The SO_2 capture capacity of CeO_2 based materials was investigated at low temperature conditions.[13–15] Manganese dioxide with a simple sulfate reaction path ($MnO_2 + SO_2 \rightarrow MnSO_4$) showed high SO_2-capture capacity at low temperature conditions.[16] The MnO_2 with high specific surface area had the potential to be more compact for disposable SO_2 traps on account of high desulfurization SO_2-capture performance at low temperature conditions. Li *et al.*[17] investigated the SO_2 capture capacity of manganese oxide at 325 °C

[a]*Key Laboratory of Renewable Energy, Guangzhou Institute of Energy Conversion, Chinese Academy of Sciences, No. 2 Nengyuan Rd. Wushan, Tianhe District, Guangzhou 510640, P. R. China. E-mail: huanghy@ms.giec.ac.cn; Fax: +86-20-37210762; Tel: +86-20-37210762*

[b]*University of Chinese Academy of Sciences, Beijing 100049, PR China*

[c]*Kanazawa University, Kakuma, Kanazawa, Ishikawa 920-1192, Japan*

[d]*Nagoya University, Furo-cho, Chikusa-ku, Nagoya 464-8603, Japan. E-mail: junli@energy.gr.jp; Fax: +81-52-7895428; Tel: +81-52-7895486*

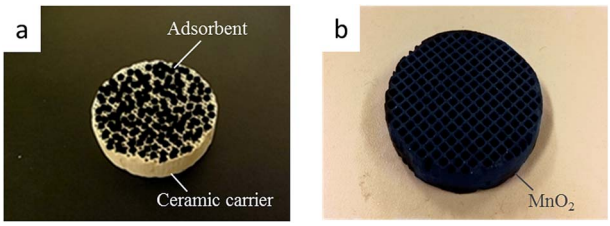

Fig. 1 Photograph of traditional filter (a) and MnO_2 filter (b).

and found that cryptomelane could be application as a replaceable absorbent for the removal of SO_2 from diesel exhaust.

Traditionally, the materials were wash-coated on ceramic carrier (Fig. 1a) by using the binder for final application in the diesel vehicle exhaust system.[18–20] The SO_2 capture capacity per unit volume of desulfurization filter greatly decreased because the ceramic carrier with low SO_2-capture performance occupied too much volume of the filter. Moreover, as the sulfur concentration of diesel is very small (a few hundred ppm), the mutual diffusion resistance could be large, which will greatly lower the diffusion rate of SO_2 reaction gas from the external air to the sites of the reactant.[21] Therefore, in this study, the compact dry desulfurization filter without ceramic carrier (MnO_2 filter) was developed to downsize the desulfurization filter, as shown in Fig. 1b, and the volumetric method was proposed to exclude the mutual diffusion resistance to obtain the real SO_2-capture behavior of compact MnO_2 filter. The effects of the reaction temperature and thickness of MnO_2 filter were investigated at low SO_2 pressure condition. The sulfate reaction mechanism between the MnO_2 filter and pure SO_2 was also discussed under four reaction temperature conditions for improving the efficiency of designing MnO_2 filter.

Experimental

MnO_2 filter preparation

50 mg MnO_2 was blended with 5 mg Carboxymethyl Cellulose (CMC) in the beaker. Exactly 2 mL of silica-sol (3.4 w% in H_2O) was added dropwise and mixed the blender by glass rod. Then, the blender was extruded through the metal mold and calcined at 400 °C to form a rounded compact MnO_2 filter. The MnO_2 used for experiments was supplied by Japan Material and Chemical Co., Ltd. These materials were obtained by the acid treatment of raw material. The chemicals, CMC and silica sol (34 w% suspension in H_2O), were purchased from Aladdin Co., Ltd., People's Republic of China and were of analytical reagent grade.

Characterization

Morphology of the sample was analyzed by using transmission electron microscope (TEM). In this study, specific surface area, average pore diameter and pore volume were conducted to assess the physical characteristics of the target sample. The specific surface area was measured by the Brunauer–Emmett–Teller with the nitrogen adsorption uptake at the boiling point of nitrogen of 77 K using a capacitive measurement method. The average pore diameter and pore volume were measured by nitrogen physisorption under normal relative pressure of 0.1–1.0 using the Barrett–Joyner–Halenda (BJH) method. The particle size distribution of the sample was analyzed by Malvern laser particle size analyzer.

Volumetric measurements

The volumetric test-rig consists mainly of two compartments, as depicted in Fig. 2. The first is sample cell, in which a sample of 0.1 g rounded absorbent is placed. The reaction temperature of sample cell can be adjusted and controlled by using the heater cover. The second compartment is a large constant volume tank. The temperature of this tank is controlled by using a thermostatic chamber.

The volumetric test-rig was used in this study to measure the SO_2 capture capacity of the prepared absorbent. Table 1 presents the experimental conditions used in the present study. The MnO_2 filter was placed into the sample cell and slowly heated (5 K min^{-1}) to the target reaction temperature. At the same time, the tank and sample was evacuated for 1 h by using the vacuum 1 with the valves V1–V3 opened. After the pressure was below 10^{-2} Pa, the valves V1–V3 were closed. The valves V4 & V2 were slowly opened to put the SO_2 gas into the tank and then closed when the pressure of the SO_2 gas was up to 40 Pa (equivalent to the partial pressure of 400 ppm SO_2 in the exhaust). The temperature of thermostatic chamber was kept at 35 °C. The sulfate reaction process started once the valve V1 was opened, leading to decreasing the pressure in the tank. The pressure

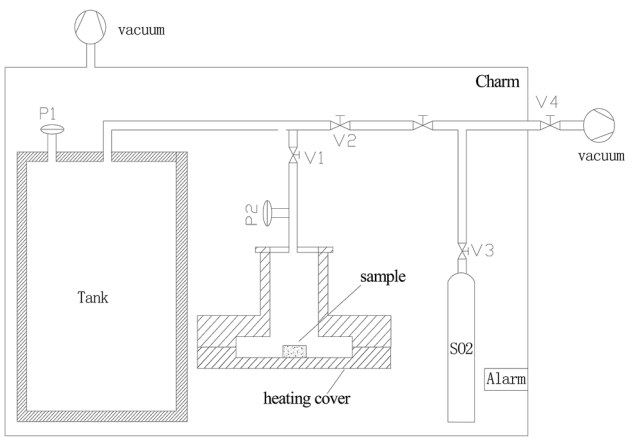

Fig. 2 Schematic diagram of the volumetric test-rig.

Table 1 Experimental conditions

Variables	Conditions
Temperature of the thermostatic chamber (K)	308
Temperature of the sample (K)	473–673
Pressure of tank (Pa)	40
Mass of the sample (g)	0.05–0.15
Thickness of the absorbent sample (mm)	0.5–2

variation was measured to determine the amount of the SO_2 gas on the sorbent sample by using the high resolution ceramic capacitance manometer P2. The SO_2 capture capacity per unit mass of absorbent C and the conversion of MnO_2 X are expressed by the following equations:

$$C = \frac{(P_0 - P)_t V}{RT} \frac{M_{SO_2}}{s_0} \left[g_{SO_2} \text{ per } g_{material}\right] \quad (1)$$

$$X = \frac{M_{MnO_2}}{M_{SO_2}} \frac{C}{\omega s_0} \left[g_{SO_2} \text{ per } g_{MnO_2}\right] \quad (2)$$

C is the SO_2 capture performance per unit mass [g_{SO_2} per $g_{material}$], R is the ideal gas constant, V is the volume of the SO_2 gas, P_0 is the initial pressure of the absorbent [Pa], P_t is the pressure after t seconds [Pa], s_0 is the initial weight of the absorbent [mg]; X is the conversion of MnO_2, ω is the mass fraction of MnO_2 in the absorbent, M_{MnO_2} is the molar mass of MnO_2 [g mol^{-1}], M_{SO_2} is the molar mass of SO_2 [g mol^{-1}].

Results and discussion

Material characterization

The distribution of pore diameter of the prepared sample is displayed in Fig. 3. From the results of Fig. 3, the relatively large pore diameter of the sample is about 7 nm. The specific surface area, average pore diameter and pore volume of the prepared sample are 275 $m^2 g^{-1}$, 7.5 nm and 0.5 $cm^3 g^{-1}$, respectively. The relatively large particle diameter of the sample is about 1.6 μm. XRD analysis (Fig. 4) is carried out to study the crystal structure of MnO_2 filter before and after desulfurization. From the results of Fig. 4, the diffraction peaks of MnO_2 filter are similar to those of tetragonal phase MnO_2 (JCPDS 00-044-0141), and after desulfurization the diffraction peaks of the sample are changed to the orthorhombic phase $MnSO_4$ (JCPDS 00-011-0088).

Basic SO_2-capture performance of MnO_2 filter by using volumetric device

Fig. 5 shows the effect of desulfurization temperature on SO_2 capture capacity of MnO_2 filter. The SO_2 capture capacity of

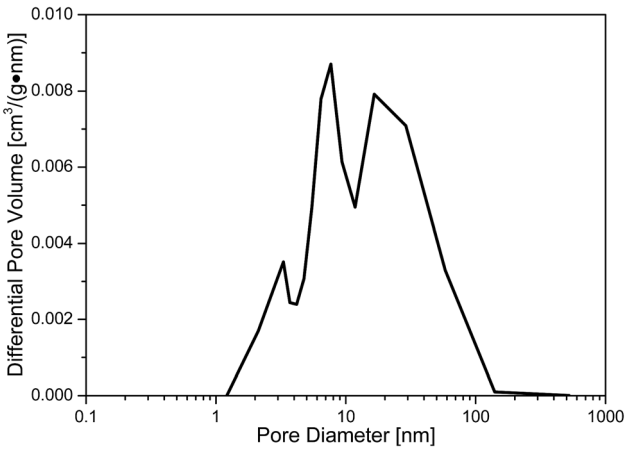

Fig. 3 Distribution of pore diameter of the prepared sample.

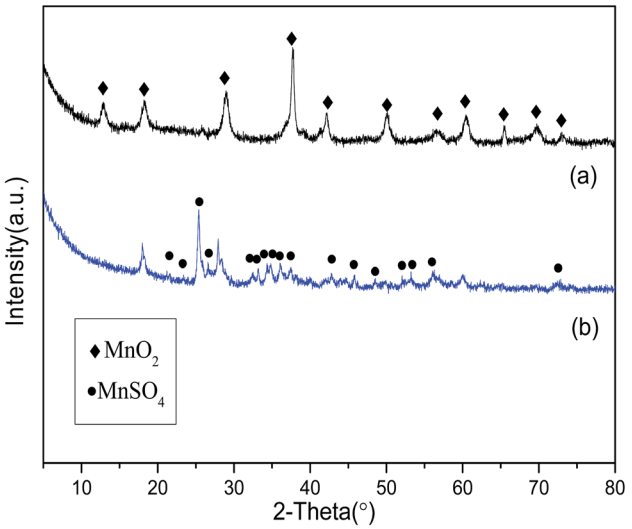

Fig. 4 XRD patterns of MnO_2 filter (a) before and (b) after desulfurization.

MnO_2 filter was investigated at 200 °C, 300 °C, 350 °C and 400 °C. From the results shown in Fig. 5, the SO_2 capture capacity of MnO_2 filter increases with the experimental temperature. At these experimental conditions, the trap achieves the highest SO_2 capture capacity and obtained about 76.3 mg_{SO_2} per g_{MnO_2} after 1 h at 400 °C. At 200 °C, the SO_2 trap capacity decreased to about 20% of its capacity at 400 °C and

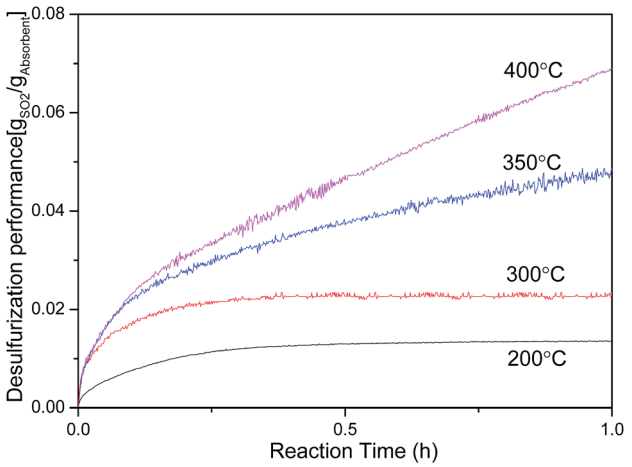

Fig. 5 Influence of temperature on SO_2 capture performance of MnO_2 filter at 200 °C, 300 °C, 350 °C and 400 °C.

Table 2 SO_2 capture capacity (mg_{SO_2} per g_{MnO_2}) of MnO_2 filter at 200–400 °C, 40 Pa pure SO_2

Reaction temperature	200 °C	300 °C	350 °C	400 °C
After adsorption 1 h	15.0	25.7	52.7	76.3
Maximal capacity	15.0	25.7	71.7	304.1

obtained 15.0 mg_{SO_2} per g_{MnO_2}. SO_2 capture capacity (mg_{SO_2} per g_{MnO_2}) of MnO_2 filter at 40 Pa pure SO_2 under different sulfate reaction temperature conditions has been listed in Table 2. As seen in the results of Table 2, the maximal capacity of MnO_2 filter was 304.1 mg_{SO_2} per g_{MnO_2} at 400 °C, significantly higher than the traditional desulfurization materials,[14,17,22] as shown in Table 3.

Based on the experimental results, the optimum volume of the MnO_2 filter required for a diesel engine was estimated. A diesel car (traveled distance: about 30 000 km of one year) is considered in which the concentrations of sulfur in the diesel oil and in lubricating oil are both 30 ppm. It is assumed that the SO_2-capture capacity is not affected by the initial sulfur concentration in this evaluation. Fuel consumption of the diesel car is 7 liter per hundred kilometers. The specific gravity of diesel oil is 0.83 kg L^{-1}. The amount of discharged SO_2 for one year is 104.6 g. Based on the evaluation that the SO_2 capture capacity at a reaction temperature of 400 °C is 182.5 g_{SO_2} per $L_{MnO_2\ filter}$ (SO_2 capture performance is 304.1 mg_{SO_2} per g_{MnO_2} at 400 °C and the density of MnO_2 filter is 0.6 g cm^{-3}), this means that a 1.0 L MnO_2 filter can capture 182.5 g of SO_2. Therefore, the required volume of the MnO_2 filter was calculated as only 0.6 L for a diesel vehicle with 30 000 km traveled distance per one year, remarkably smaller than the traditional wash-coated desulfurization filter.[7] Morever, as a part of the storage sites on MnO_2 after regeneration are non-renewable[16] and the desulfurization product ($MnSO_4$) is always in great demand for the industrial and agricultural raw material, MnO_2 filter could be suitable for the disposable desulfurization filter without being recycled every year for economy.[23]

The effect on SO_2 capture capacity of MnO_2 filter with different thickness

In the traditional SO_2 traps,[4] the amount of SO_2 capture was dependent on the quantity of sorbents in the desulfurization trap. In this study, similar experimental results were obtained. The amount of SO_2 adsorption was proportional to the thickness of MnO_2 filter, as shown in Fig. 6. The thickness of

Table 3 SO_2 capture capacity (mg_{SO_2} per $g_{material}$) of some investigated materials

Materials	SO_2 capture capacity	Reaction conditions	References
MnO_2 filter	304.1	400 °C, 40 Pa pure SO_2	In present work
$CuO–CeO_2$	24	400 °C, 3600 ppm SO_2	Rodas-Grapaín *et al.*[14]
TO-AC	161	400 °C, 2000 ppm SO_2	Guo *et al.*[22]
$Pt–Pd–Al_2O_3$	11	600 °C, 30 ppm SO_2	Limousy *et al.*[4]
CaO	36	325 °C, 250 ppm SO_2	Li *et al.*[17]
$Ca(OH)_2$	32	325 °C, 250 ppm SO_2	Li *et al.*[17]
MgO	20	325 °C, 250 ppm SO_2	Li *et al.*[17]
ZrO_2	16	325 °C, 250 ppm SO_2	Li *et al.*[17]
CuO-AC	30	250 °C, 200 ppm SO_2	Tseng *et al.*[12]
Coal fly ash	13	100 °C, 1000 ppm SO_2	Rubio and Izquierdo[10]

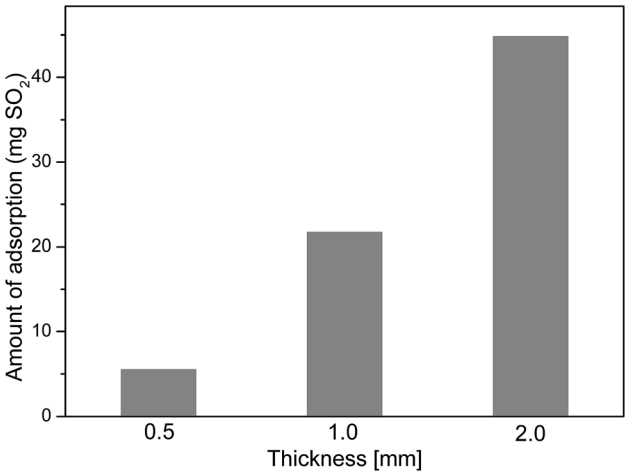

Fig. 6 Effect of the thickness of the MnO_2 filter on the amount of SO_2 adsorption.

materials had much influence on the removal performance of diesel exhaust purifier.[24] The dimensionless SO_2 capture performance per unit mass (mg_{SO_2} per g_{MnO_2})–time (t) curve of MnO_2 filter with different thickness was obtained by using the volumetric test-rig. As shown in Fig. 7, the shape of the curve is different when the packing height is changed. The SO_2 capture rate of MnO_2 filter decreased with the thickness. The 0.5 mm-thick MnO_2 filter showed the highest SO_2 capture rate than 2 mm-thick MnO_2 filter. The reason is that the mass transfer resistance of gas diffusion in the thicker layer is larger than that in the thinner layer in the adsorbent.[7]

Sulfate reaction mechanism

The sulfate reaction mechanism is very important for improving the efficiency of designing the desulfurization filter. In this study, in order to investigate the sulfate reaction mechanism between MnO_2 filter and sulfur dioxide, the MnO_2 filter with thin layer and low density was prepared to minimize the gas

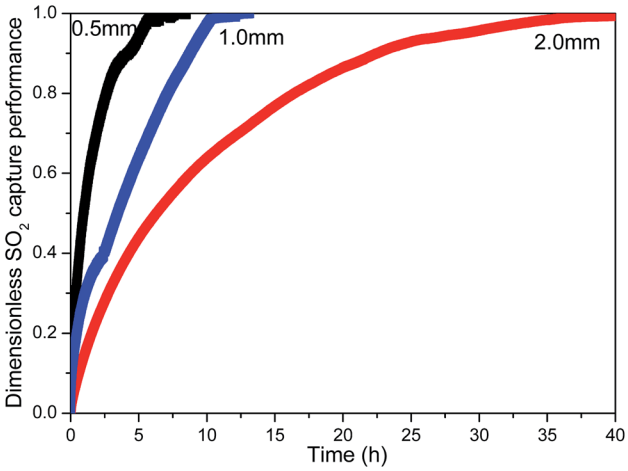

Fig. 7 Effect of the thickness of the MnO_2 filter on the SO_2 adsorption performance.

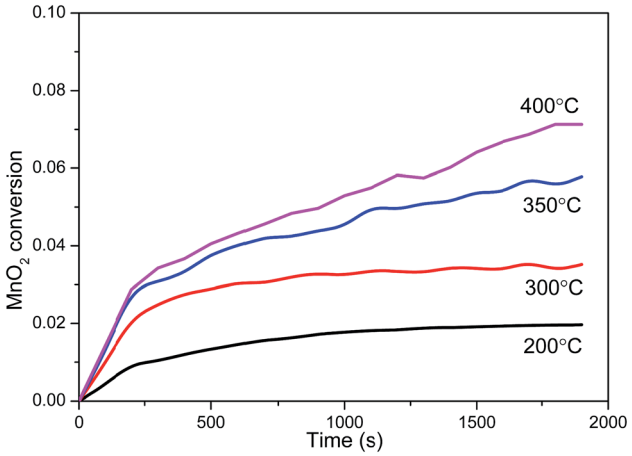

Fig. 8 Effect of temperature on solid conversion of MnO_2 filter at 40 Pa of SO_2 gas pressure.

diffusion resistance in the traps. Moreover, a series of experiments were carried out at four reaction temperature conditions (200 °C, 300 °C, 350 °C and 400 °C) with low SO_2 pressure of 40 Pa. Fig. 8 shows the conversion-time profiles of MnO_2 filter for different temperature at low SO_2 pressure of 40 Pa. As this figure shows, the reaction rate increases considerably at higher temperatures. The sulfate degree in the experimental conditions increased steeply at the beginning of the reaction, and then the slopes of sulfate degree curves become gradual after ~5 min.

The sulfate reaction between manganese dioxide and sulfur dioxide with a simple reaction path ($MnO_2 + SO_2 \rightarrow MnSO_4$) is a solid–gas non-catalytic reaction. Various models had been discussed to describe the mechanism of the solid–gas non-catalytic reaction.[25] Among these models, the grain model was a suitable mathematical representation of gas–solid reactions in chemical and metallurgical industries consist of solid pellets produced from small particles or grains, which assumes that the reaction was accomplished on the surface of the fine and non-porous grains.[26] TEM were employed to obtain surface features of the samples before and after desulfurization, the results as shown in the Fig. 9. Based on the TEM images in Fig. 9, the prepared MnO_2 filter was formed with a series of smooth spherical grains and these grains are non-porous. Therefore, the grain model should be suitable for the solid–gas reaction between MnO_2 filter and SO_2.

In the grain model, the sulfate rate is controlled by four steps: external diffusion, gas reactant diffusion to the external surfaces of the solid particles from the bulk gas phase; surface reaction, gas reactant being adsorbed on the solid reactant surface; solid diffusion, gas reactant diffusion through the product layers; internal diffusion, gas reactant intra-particle transport through pores. For the whole systems, the controlling regime changes with the reaction time and was continuously consumed because the solid is a reactant.[27] Most solid–gas non-catalytic reactions always presented two consecutive stages: the initial stage with the fast sulfate rate was controlled by the surface chemical reaction; the second stage with the slower sulfate rate was controlled by the product layer diffusion.[28,29] According to the grain model, the relationship between the solid conversion equation X and the reaction time t at the chemical reaction control stage for the spherical particle and grain can be expressed by the following equation:

$$t = \frac{\rho_s r_g}{b k_s C_A}\left[1 - (1 - X)^{1/3}\right] \quad (3)$$

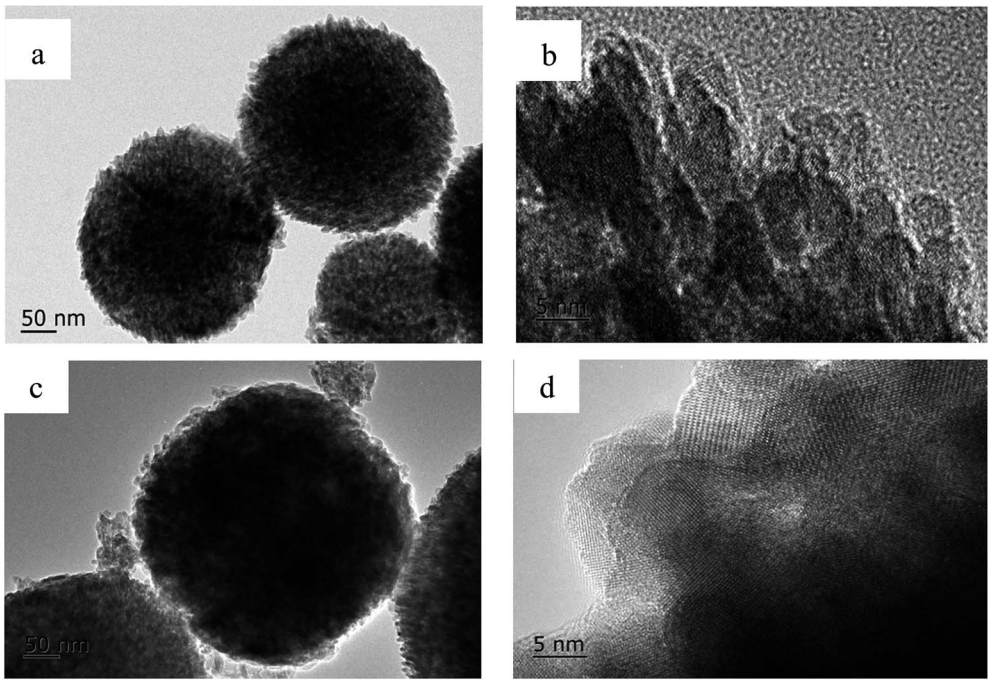

Fig. 9 TEM images of MnO_2 filter before (a, b) and after desulfurization (c, d).

where ρ_s is the solid reactant concentration, k_s is the surface chemical reaction rate constant, C_A is the concentration of reactant gas, b is the stoichiometric coefficient of the reaction, r_g is the initial radius of the spherical grain, X the conversion of solid reactant. The relationship between the solid conversion equation X and the reaction time t at the solid diffusion control stage for the spherical particle and grain can be expressed by the following equation:

$$t = \frac{\rho_s {r_g}^2}{6bkD_e C_A}\left[t_0 + 1 - 3(1-X)^{2/3} - 2(1-X)\right] \quad (4)$$

where D_e is the effective diffusivity, t_0 is the revision factor of the delay time for sulfate rate from the chemical reaction control stage to solid diffusion control stage.

The grain model prediction of chemical reaction control, expressed in eqn (3), was applied to curve-fitting for the beginning of the sulfate process (the initial stage); and the grain model prediction of solid diffusion control, expressed in eqn (4), was applied to fit experimental data for the increase reaction time of sulfate process (the second stage). Fig. 10 shows the lines of the model predictions of chemical reaction control and solid diffusion control under the different reaction temperature conditions. From the results shown in Fig. 10, it can be seen that the prediction models fit the experimental data well for both control stages at 200 °C and 300 °C. At 350 °C and 400 °C, the prediction model of chemical reaction control fit the experimental data well at the initial stage of sulfate process. At higher temperature, the sulfate rate was controlled the zone of sulfate reaction between porous solid and gas became a relative narrow with the sulfate reaction proceeding and the surface reaction rate and diffusion rate were of the same order of magnitude.[30] Therefore, the sulfate rate could be controlled by the chemical reaction and solid diffusion at the second stage at 350 °C and 400 °C. Generally, it can be safely concluded that the grain model is suitable for the solid–gas reaction between MnO_2 filter and SO_2 and the sulfate process could be divided into two control stages (the chemical reaction control stage and the solid diffusion control stage) under the experimental conditions.

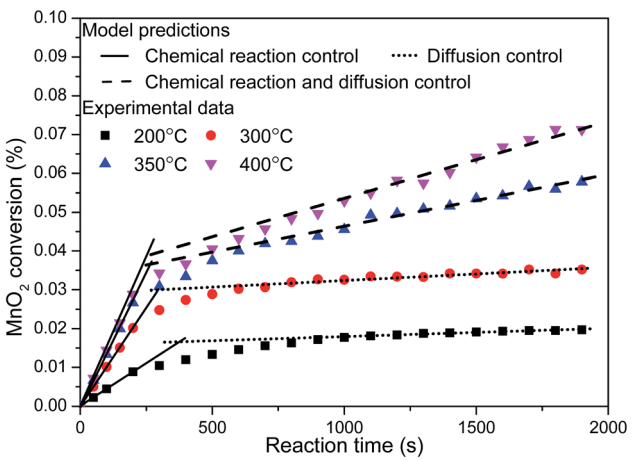

Fig. 10 Experimental data and model predictions of MnO_2 conversion under four reaction temperature conditions.

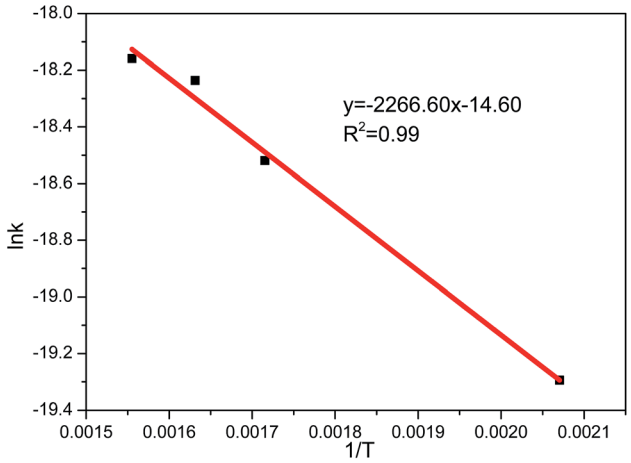

Fig. 11 Arrhenius plot of sulfate rate of MnO_2 filter with chemical reaction control.

In order to determine the activation energy of the sulfate reaction between the MnO_2 filter and pure SO_2, the sulfate reaction rate constant of the chemical reaction control stage was measured at 200 °C, 300 °C, 350 °C and 400 °C. The corresponding Arrhenius plot is shown in Fig. 11. The apparent activation energy of 18.8 kJ mol^{-1} was calculated by using Arrhenius equation under the experimental conditions. Compared with the value of sulfate reaction of manganese oxide (33.5 kJ mol^{-1}) reported by Tikhomirov,[31] it can be concluded that in the pure SO_2 atmosphere the MnO_2 filter exhibits high activity for SO_2 adsorption.

Conclusions

MnO_2 filter is used for compact SO_2 trap to protect the NO_x removal catalyst against SO_2 poisoning in diesel exhaust system. The SO_2-capture performance of MnO_2 filter without mutual diffusion resistance was measured by volumetric method under low temperature and low SO_2 pressure conditions. MnO_2 filters with different thickness and packing density were prepared, and the influences of reaction temperature, thickness of MnO_2 filter and recycling characteristic of MnO_2 filter on SO_2 capture capacity were investigated under low temperature range from 200 °C to 400 °C and low SO_2 pressure of 40 Pa conditions. The results of the present work clearly reveal that:

- The maximal capacity of MnO_2 filter was 304.1 mg_{SO_2} per g_{MnO_2} at 400 °C. The required volume of the MnO_2 filter was estimated as only 0.6 L for a diesel car with 30 000 km traveled distance per one year and MnO_2 filter could be suitable for the disposable desulfurization filter.
- The 0.5 mm-thick MnO_2 filter showed the higher SO_2 capture rate than 2 mm-thick MnO_2 traps because the mass transfer resistance in the thicker layer was larger than that in the thinner layer.
- The grain model is suitable for the sulfate reaction, and the sulfate process can be divided into two control stages (the chemical reaction control stage and the solid diffusion control stage). The prediction models fit the experimental data well for

both control stages. The apparent activation energy of 18.8 kJ mol^{-1} was calculated by using Arrhenius equation under the experimental conditions, which exhibits high sulfate activity between the MnO_2 filter and pure SO_2.

Acknowledgements

This research was supported by National Natural Science Foundation of China (NSFC) through International (Regional) Cooperation and Exchange Projects (Grant No. 21550110494) and Chinese Academy of Sciences President's International Fellowship Initiative (Grant No. 2016VTC068).

References

1 J. Ding, Q. Zhong and S. Zhang, Simultaneous removal of NO_x and SO_2 with H_2O_2 over Fe based catalysts at low temperature, *RSC Adv.*, 2014, **4**(11), 5394–5398.
2 H. Moshiri, B. Nasernejad, H. Ale Ebrahim and M. Taheri, Solution of coupled partial differential equations of a packed bed reactor for SO_2 removal by lime using the finite element method, *RSC Adv.*, 2015, **5**(23), 18116–18127.
3 R. Y. Jiang, H. H. Shan, Q. Zhang, C. Y. Li and C. H. Yang, The influence of surface area of De-SO_x catalyst on its performance, *Sep. Purif. Technol.*, 2012, **95**, 144–148.
4 L. Limousy, H. Mahzoul, J. F. Brilhac, P. Gilot, F. Garin and G. Maire, SO_2 sorption on fresh and aged SO_x traps, *Appl. Catal., B*, 2003, **42**(3), 237–249.
5 X. C. Liu, Y. Osaka, H. Y. Huang, *et al.*, Development of low-temperature desulfurization performance of a MnO_2/AC composite for a combined SO_2 trap for diesel exhaust, *RSC Adv.*, 2016, **6**(98), 96367–96375.
6 Y. Osaka, T. Kito, N. Kobayashi, S. Kurahara, H. Huang, H. Yuan and Z. He, Removal of sulfur dioxide from diesel exhaust gases by using dry desulfurization MnO_2 filter, *Sep. Purif. Technol.*, 2015, **150**, 80–85.
7 Y. Osaka, Y. Kohei, T. Tsujiguchi, A. Kodama, H. Huang and Z. He, Study on the Optimized Design of DeSO_x Filter Operating at Low Temperature in Diesel Exhaust, *J. Chem. Eng. Jpn.*, 2014, **47**, 555–560.
8 R. H. Borgwardt, Kinetics of the reaction of sulfur dioxide with calcined limestone, *Environ. Sci. Technol.*, 1970, **4**(1), 59–63.
9 Y. Osaka, S. Kurahara, N. Kobayashi, M. Hasatani and A. Matsuyama, Study on SO_2-Absorption Behavior of Composite Materials for De$SO(x)$ Filter From Diesel Exhaust, *Heat Transfer Eng.*, 2015, **36**(3), 325–332.
10 B. Rubio and M. T. Izquierdo, Coal fly ash based carbons for SO_2 removal from flue gases, *Waste Manage.*, 2010, **30**(7), 1341–1347.
11 H. H. Tseng and M. Y. Wey, Study of SO_2 adsorption and thermal regeneration over activated carbon-supported copper oxide catalysts, *Carbon*, 2004, **42**(11), 2269–2278.
12 H. H. Tseng, M. Y. Wey and C. H. Fu, Carbon materials as catalyst supports for SO_2 oxidation: catalytic activity of CuO-AC, *Carbon*, 2003, **41**(1), 139–149.
13 K. Tikhomirov, O. Kröcher, M. Elsener and A. Wokaun, MnO_x–CeO_2 mixed oxides for the low-temperature oxidation of diesel soot, *Appl. Catal., B*, 2006, **64**(1–2), 72–78.
14 A. Rodas-Grapaín, J. Arenas-Alatorre, A. Gómez-Cortés and G. Díaz, Catalytic properties of a CuO–CeO_2 sorbent-catalyst for De-SO_x reaction, *Catal. Today*, 2005, **107–108**, 168–174.
15 Z. Yan, J. P. Wang, R. Q. Zou, L. L. Liu, Z. T. Zhang and X. D. Wang, Hydrothermal Synthesis of CeO_2 Nanoparticles on Activated Carbon with Enhanced Desulfurization Activity, *Energy Fuels*, 2012, **26**(9), 5879–5886.
16 X. Liu, Y. Osaka, H. Huang, A. Kodama, Z. He, Huhetaoli, X. Yang and Y. Chen, Development of high-performance SO_2 trap materials in the low-temperature region for diesel exhaust emission control, *Sep. Purif. Technol.*, 2016, **162**, 127–133.
17 L. Y. Li and D. L. King, High-capacity sulfur dioxide absorbents for diesel emissions control, *Ind. Eng. Chem. Res.*, 2005, **44**(1), 168–177.
18 E. Tronconi and A. Beretta, The role of inter- and intra-phase mass transfer in the SCR-DeNO_x reaction over catalysts of different shapes, *Catal. Today*, 1999, **52**(2–3), 249–258.
19 C. Orsenigo, A. Beretta, P. Forzatti, J. Svachula, E. Tronconi, F. Bregani and A. Baldacci, Theoretical and experimental study of the interaction between NOx reduction and SO_2 oxidation over DeNO_x-SCR catalysts, *Catal. Today*, 1996, **27**(1), 15–21.
20 J. Blanco, P. Avila, A. Bahamonde, M. Yates, J. L. Belinchón, E. Medina and A. Cuevas, Influence of the operation time on the performance of a new SCR monolithic catalyst, *Catal. Today*, 1996, **27**(1), 9–13.
21 O. L. Lange and J. D. Tenhunen, Moisture content and CO_2 exchange of lichens. II. Depression of net photosynthesis in Ramalina maciformis at high water content is caused by increased thallus carbon dioxide diffusion resistance, *Oecologia*, 1981, **51**(3), 426–429.
22 J. X. Guo, L. Fan, J. F. Peng, J. Chen, H. Q. Yin and W. J. Jiang, Desulfurization activity of metal oxides blended into walnut shell based activated carbons, *J. Chem. Technol. Biotechnol.*, 2014, **89**(10), 1565–1575.
23 G. Centi and S. Perathoner, Dynamics of SO_2 adsorption–oxidation in SO_x traps for the protection of NO_x adsorbers in diesel engine emissions, *Catal. Today*, 2006, **112**(1–4), 174–179.
24 I. Binder-Begsteiger, Improved emission control due to a new generation of high-void-fraction SCR-DeNO_x catalysts, *Catal. Today*, 1996, **27**(1), 3–8.
25 A. Gómez-Barea and P. Ollero, An approximate method for solving gas–solid non-catalytic reactions, *Chem. Eng. Sci.*, 2006, **61**(11), 3725–3735.
26 A. A. Ebrahimi, H. A. Ebrahim, M. Hatam and E. Jamshidi, Finite element solution for gas–solid reactions: application to the moving boundary problems, *Chem. Eng. J.*, 2008, **144**(1), 110–118.
27 F. Fang, Z. Li, N. Cai, X. Tang and H. Yang, AFM investigation of solid product layers of $MgSO_4$ generated

on MgO surfaces for the reaction of MgO with SO_2 and O_2, *Chem. Eng. Sci.*, 2011, **66**(6), 1142–1149.

28 P. Sun, J. R. Grace, C. J. Lim and E. J. Anthony, The effect of CaO sintering on cyclic CO_2 capture in energy systems, *AIChE J.*, 2007, **53**(9), 2432–2442.

29 J. S. Dennis and R. Pacciani, The rate and extent of uptake of CO_2 by a synthetic, CaO-containing sorbent, *Chem. Eng. Sci.*, 2009, **64**(9), 2147–2157.

30 C. Y. Wen and M. Ishida, Reaction rate of sulfur dioxide with particles containing calcium oxide, *Environ. Sci. Technol.*, 1973, **7**(8), 703–708.

31 K. Tikhomirov, O. Krocher, M. Elsener, M. Widmer and A. Wokaun, Manganese based materials for diesel exhaust SO_2 traps, *Appl. Catal., B*, 2006, **67**(3–4), 160–167.